JOURNAL OF MAGNETIC RESONANCE 67, 258–266 (1986)

FLASH Imaging. Rapid NMR Imaging Using Low Flip-Angle Pulses

A. HAASE, J. FRAHM, D. MATTHAEI, W. HÄNICKE, AND K.-D. MERBOLDT

Max-Planck-Institut für biophysikalische Chemie, Postfach 2841, D-3400 Göttingen, Federal Republic of Germany

Received October 2, 1985; revised November 12, 1985

A new method for rapid NMR imaging dubbed FLASH (*f*ast *l*ow-*a*ngle *sh*ot) imaging is described which, for example, allows measuring times of the order of 1 s (64 × 128 pixel resolution) or 6 s (256 × 256 pixels). The technique takes advantage of excitation pulses with small flip angles eliminating the need of waiting periods in between successive experiments. It is based on the acquisition of the free induction decay in the form of a gradient echo generated by reversal of the read gradient. The entire imaging time is only given by the number of projections desired times the duration of slice selection and data acquisition. The method results in about a 100-fold reduction in measuring time without sacrificing spatial resolution. Further advantages are an optimized signal-to-noise ratio, the applicability of commercial gradient systems, and the deposition of extremely low rf power. FLASH imaging is demonstrated on phantoms, animals, and human extremities using a 2.3 T 40 cm bore magnet system. ^{1}H NMR images are obtained with variable relaxation time contrasts and without motional artifacts.

INTRODUCTION

Spatially resolved nuclear magnetic resonance techniques are now extensively used for noninvasive investigations of living matter in biology and medicine (*1*). However, measuring times of several minutes lead to motional artifacts within NMR images and give no access to the study of fast physiological processes. More rapid techniques are either limited in spatial resolution or signal-to-noise ratio (SNR) (*2*), or require the application of a large number of intense radiofrequency (rf) excitation pulses (*3*) exceeding safety guidelines (*4*) at magnetic field strengths of 1 to 2 T. The first rapid imaging technique applicable to high-field imaging is rapid stimulated-echo imaging (STEAM) (*5*). Although the method inherently has the advantages of the STEAM imaging method (*6*) such as giving access to rapid T_1 images or CHESS (chemical shift selective) images, it suffers from low SNR. This is mainly because subsequently excited stimulated echoes are attenuated by T_1 relaxation.

Here we present a new rapid imaging technique dubbed FLASH (*f*ast *l*ow-*a*ngle *sh*ot) imaging, which results in (i) optimized SNR, (ii) about a 100-fold reduction of the measuring time, (iii) no loss of spatial resolution, and (iv) low rf power deposition (*7, 8*). Since the FLASH sequence works continuously without internal waiting times, one may choose arbitrary compromises between spatial resolution, time resolution, and SNR. In addition, one may record sequential series of images ("movies") with image repetition times given by the individual measuring times.

0022-2364/86 $3.00

METHOD

NMR imaging experiments are based on the acquisition of free induction decays (*9*), spin echoes (*10*), or stimulated echoes (*6*). Since the FID requires only a single rf excitation pulse this type of signal turns out to be best-suited for rapid NMR imaging. An appropriate rf pulse and gradient sequence is shown in Fig. 1. The important difference between conventional imaging techniques and this rapid sequence is the use of rf pulses with low flip angles. Low-angle pulses have already been discussed for conventional NMR spectroscopy experiments in order to optimize the SNR per measuring time (*11, 12*). However, repetition times of the order of tens of milliseconds, i.e., flip angles of the order of 15°, have not been applied because spectroscopic FID signals normally have durations of several hundreds of milliseconds. This situation becomes different for NMR imaging where magnetic field gradients reduce the length of the FID to some milliseconds.

For example, using a flip angle of 15°, the intensity of the FID corresponds to 25% (sin 15°) of the maximum amplitude excited by a 90° pulse. In contrast to conventional imaging sequences, 96.5% (cos 15°) of the longitudinal magnetization remains unaffected and thus is available for immediate subsequent excitations (see Fig. 1). After termination of the rf pulse the slice-selective gradient (*G* slice) is inverted for proper refocusing of the transverse magnetization (*13*). The in-plane spatial discrimination may be achieved either by rotating a magnetic field gradient in a number of steps according to the projection reconstruction algorithm (*14*) or by applying a fixed "read" gradient (*G* read) and a perpendicular phase-encoding gradient (*G* phase) of variable strength according to the 2D Fourier imaging method (*15*). The read gradient is inverted prior to the data acquisition period leading to a so-called gradient or field echo. Immediately after acquisition of the data the experiment is repeated with a repetition time given by the time needed for slice selection and data acquisition. Thus the duration of the entire imaging experiment is reduced by the same factor as conventional repetition times of the order of 1 s are reduced to about 10–20 ms. After application of the first 20–40 excitation pulses, the spin system reaches a steady state where the loss

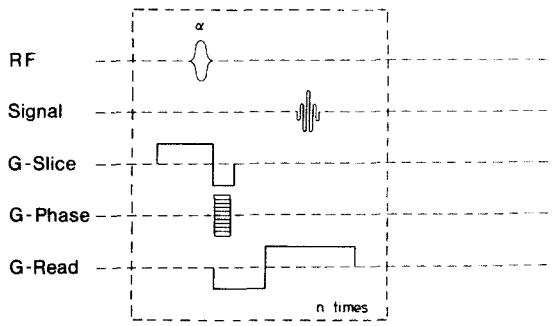

FIG. 1. Radiofrequency pulse and magnetic field gradient sequence for rapid FLASH NMR imaging. The method employs slice selective excitation pulses with flip angles of the order of 15°. The NMR free induction decay is detected in the form of a gradient echo after reversal of the read gradient. The sequence is repeated *n* times recording *n* projections with different phase-encoding gradients. No waiting times are required between subsequent excitations.

of longitudinal magnetization by excitation is compensated for by spin–lattice relaxation during the imaging sequence. The theoretical value of this steady state as well as its dependence on T_1, on the repetition time, and on the flip angle have already been discussed by Waugh (*12*). After reaching the steady state, experiments can be performed without time limits. For example, series of sequential images may be recorded describing the time course of physiological processes in tissues.

EXPERIMENTAL RESULTS

Biomedical applications of NMR imaging mainly rely on tissue contrasts due to differences in relaxation times. Obviously, new and in particular rapid NMR imaging sequences should retain this sensitivity to relaxation times. Tissue contrast in FLASH images is determined by the spin–lattice relaxation time T_1 and the effective spin–spin relaxation time $T_{2\text{eff}}$. Both effects will be experimentally demonstrated below. ^{1}H NMR images are recorded using a combined imaging/spectroscopy system supplied with a 40 cm bore 2.3 T magnet (Bruker Medizintechnik, Karlsruhe, West-Germany). The duration of the frequency-selective rf pulse (compare Fig. 1) is 2 ms. In the presence of a magnetic field gradient of strength 0.5 G/cm this pulse excites transverse magnetization of a plane of about 4 mm thickness perpendicular to the direction of the gradient. The time interval from the center of the rf pulse to the maximum of the gradient echo is about 9 ms. Prior to the recording of the first projection data we have employed dummy excitations for about 0.5 s to establish a steady-state magnetization. Dummy experiments can be avoided by adjusting the flip angles of the rf pulses such that equal amounts of transverse magnetizations are excited. Assuming an average value of T_1, this can be done by starting the experiment using low flip angles and increasing their values asymptotically to the desired steady-state value during the initial part of the imaging sequence. Since individual experiments have a duration of 18 ms, the imaging times are 1.15 and 2.3 s for a 64 × 128 image and a 128 × 128 image, respectively. 256 × 256 images may be recorded within 6 s. These imaging times may even be reduced using magnetic field gradients with higher field strengths (e.g., 2 G/cm) and/or better switching times (e.g., 1 ms or less).

Spin–Lattice Relaxation Time Contrast

FLASH imaging techniques take advantage of a high-level steady-state of the longitudinal magnetization. This level is determined by the repetition time of the rf pulses, their flip angles, and the spin–lattice relaxation time T_1. Assuming a constant measuring time, i.e., repetition time, the T_1 contrast is only dependent on the flip angle. Figure 2 demonstrates the effect of varying the flip angle from 10 to 40° (Figs. 2a–d) for a phantom with different T_1 values. For a selected T_1 value, increasing the flip angle

FIG. 2. Spin–lattice relaxation time contrast within 100 MHz ^{1}H NMR FLASH images (128 × 128 pixels corresponding to 1 mm resolution, 4 mm slice thickness, measuring time 2.3 s). The water phantom shown contains different T_1 values ranging from 2600 ms (upper row left) to 220 ms (upper row right), and 430, 860, and 1150 ms (lower row from left to right). (a–d) Images obtained with flip angles of 10, 20, 30, and 40°. (e) Same as (a) but with application of an 180° pulse immediately prior to the imaging sequence shown in Fig. 1. (f) Same as (e) but with a measuring time of 1.15 s according to a 64 × 128 pixel resolution.

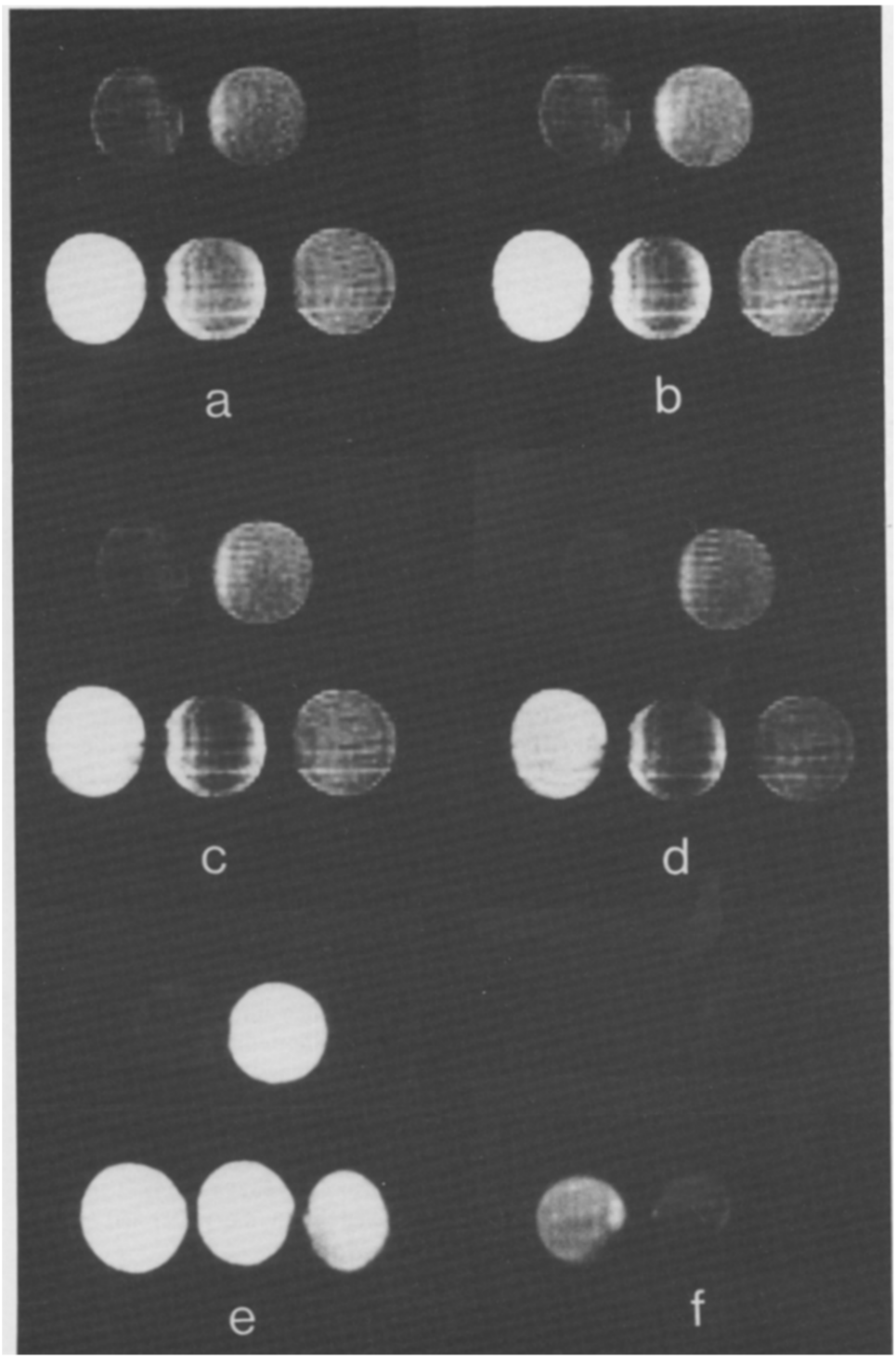
a
b
c
d
e
f

results in reduced signal intensities because of a more pronounced degree of saturation. Vice versa, for a given flip angle the intensity increases with decreasing T_1.

An additional way of enhancing T_1 contrast within FLASH images is due to the use of extra pulses, e.g., 90 or 180°, at selected positions during the imaging sequence. Since the measuring times of the rapid NMR images are of the order of the spin–lattice relaxation times, i.e., 1–2 s, even a single rf pulse will result in intensity changes. However, the point spread function along the phase-encoded direction might be changed due to imaging in the presence of a nonequilibrium state. As an example, Figs. 2e, f show the influence of a 180° pulse applied prior to the imaging sequence after termination of the dummy excitations. This pulse inverts the steady-state magnetization, so that the subsequent recovery period is probed by the FLASH imaging procedure. Depending on the imaging time the intensities of image contributions with different T_1 values are manipulated. For example, in the 2 s image shown in Fig. 2e the large water T_1 value of about 2 s is mainly affected. In addition, the 1 s image exhibits a further signal reduction of contributions with T_1 values of about 1 s leading to a strong contrast enhancement with respect to short T_1 values. In general, the accessible T_1 contrast within rapid images is about the same as within conventional NMR images, i.e., tissues with high T_1 values are represented by low intensities, while tissues with low T_1 values appear brighter.

Effective Spin–Spin Relaxation Time Contrast

Strong contrast within FLASH images is due to the attenuation of the gradient echo or FID by the effective spin–spin relaxation time $T_{2\text{eff}}$. In principle, $T_{2\text{eff}}$ reflects the occurrence of inhomogeneities of the static magnetic field either within the NMR magnet or the individual tissues. Problems of magnetic field inhomogeneities have been mainly overcome by the use of superconducting magnets, so that in the absence of gradients within the imaging object conventional T_2 contrasts are to be expected by varying the echo time. On the other hand, in the case of internal gradients in tissues *in vivo* $T_{2\text{eff}}$ contrasts give new access to structural information. This is demonstrated in Fig. 3 depicting horizontal FLASH images of the human hand at three different echo times. Using a short echo time of about 9 ms (Fig. 3a), the image appears more or less normal showing muscles, joints, marrow, vessels, and fat. However, as known from spin-echo or stimulated-echo images, the lipid signals from the bone marrow should be more intense due to their short T_1 values. Their intensity is considerably reduced because of the generation of internal gradients shortening $T_{2\text{eff}}$ mainly in the heterogeneously structured regions of the bones. In particular, the trabecular structure of the bones in the wrist and in the epiphysial parts of the metacarpalia leads to significant signal losses, whereas the lipid signals from the cavities exhibit strong intensities due to their short T_1 and relatively long T_2. These effects are even better seen in Fig. 3b using an echo time of 17 ms. In the 22 ms image shown in Fig. 3c one can already recognize the influence of B_0 inhomogeneities in the upper left part of the image.

Elimination of Motional Artifacts

NMR imaging *in vivo* often suffers from image artifacts in the direction of the phase-encoding gradient due to motions of the object under investigation. While periodic

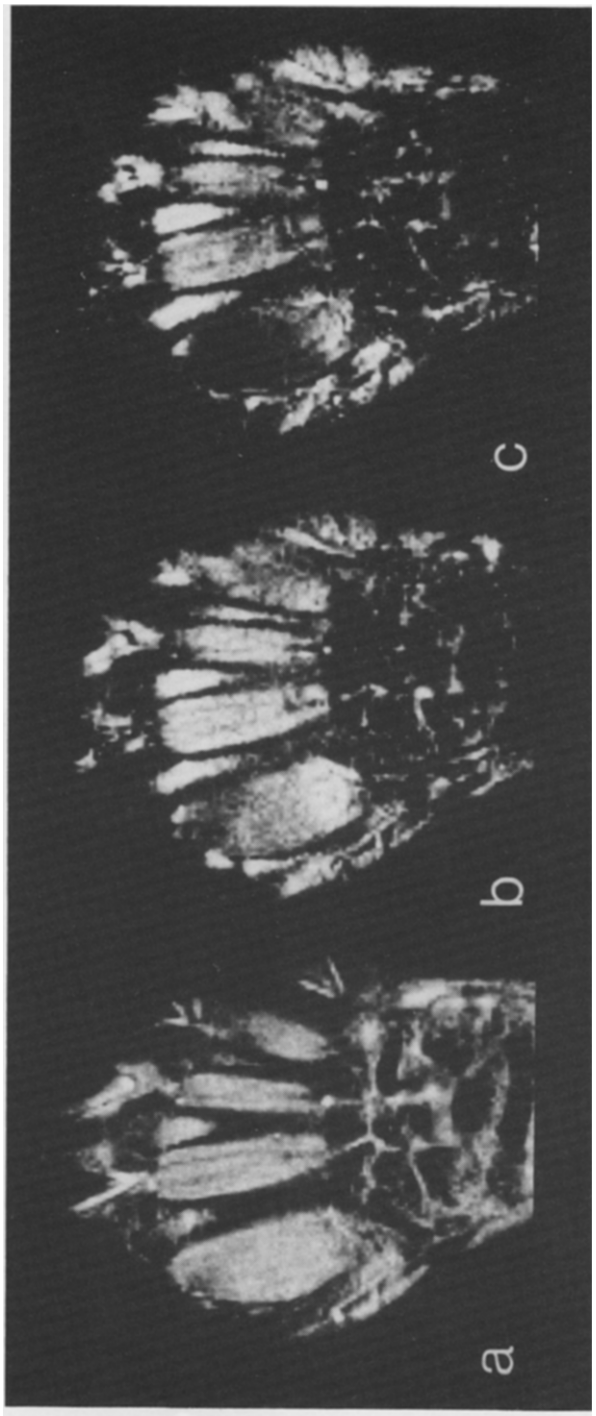

FIG. 3. Effective spin–spin relaxation time contrast within 100 MHz ^{1}H NMR FLASH images depicting a horizontal slice of the human head (128 × 128 pixels corresponding to 1 mm resolution, 4 mm slice thickness, measuring time 2.3 s). The echo times of the images, i.e., the times between the center of the rf pulses and the maximum of the gradient echoes, are (a) 9 ms, (b) 17 ms, and (c) 22 ms.

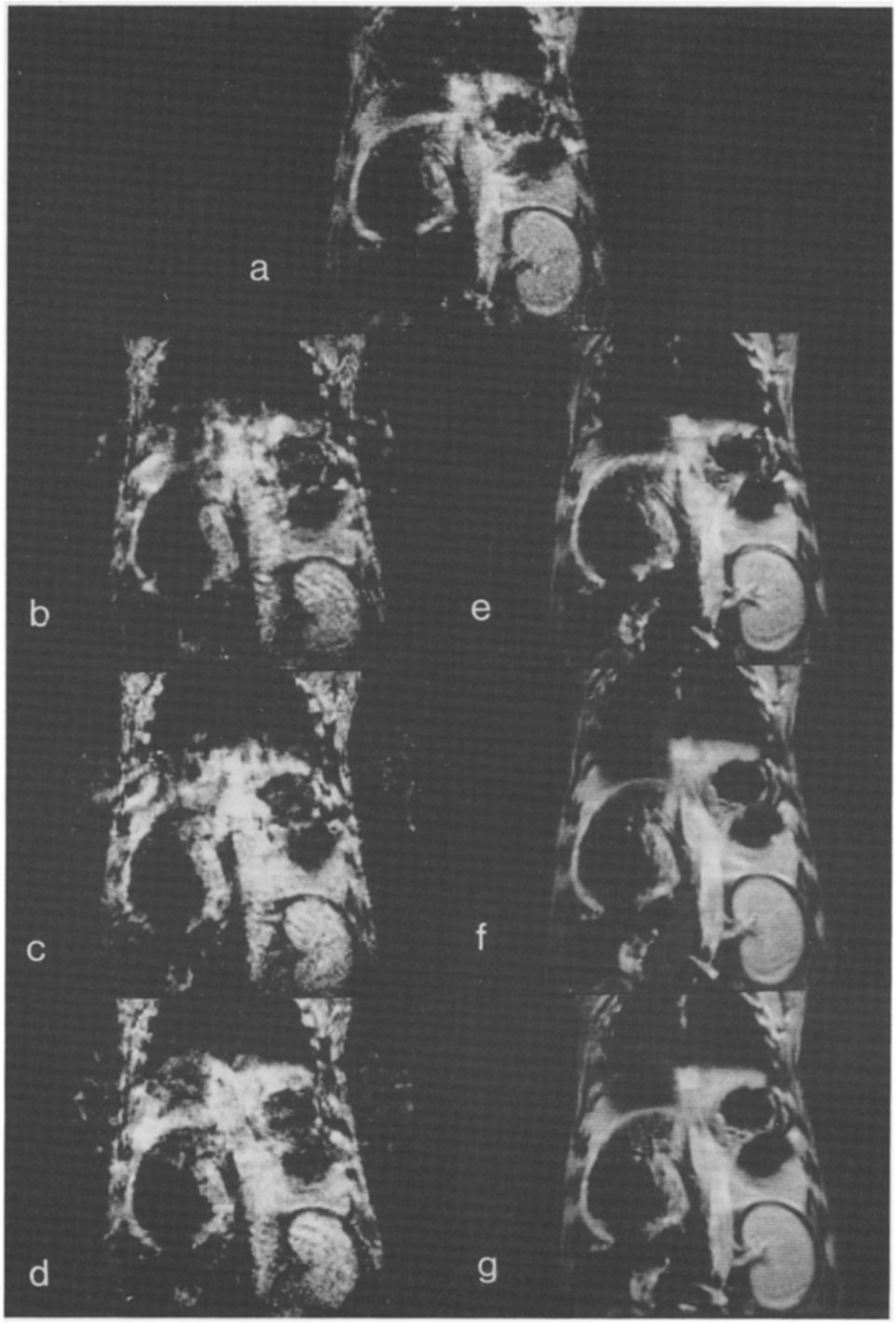
a
b
c
d
e
f
g

motions such as breathing and heart beat may be accounted for by gating or triggering techniques, artifacts due to nonperiodic motions such as peristaltic can hardly be avoided. Rapid FLASH imaging yields a simple solution to these problems. This is because fast movements with time constants of the order of the imaging time do not affect the imaging procedure. This is demonstrated in Fig. 4a for a horizontal slice through the abdomen of a live anesthesized rabbit depicting a kidney, the lungs, the diaphragm, the stomach, and parts of the liver and the dorsal mediastinum. The measuring time is 2.3 s. In Figs. 4b–d the measuring time has been increased to 9, 18, and 36 s by increasing the repetition time of the sequence. Obviously, the image quality is severely degraded.

On the other hand, averaging of accumulated FLASH images is possible to increase SNR at the expense of time resolution. This is demonstrated in Figs. 4e–g which show images with the same overall measuring time as in Figs. 4b–d. However, instead of increasing the repetition time, 4, 8, and 16 individual 2.3 s FLASH images have been summed up. Although the images exhibit some minor blurring effects, the gain in quality as compared to Figs. 4b–d is striking. It turns out that even periodic motions with time constants shorter than the measuring time may be imaged by averaging rapidly recorded FLASH images. This can be judged from the appearance of the dorsal mediastinum within Figs. 4e–g. This finding is currently explored for heart imaging without gating (*16*).

CONCLUSION

A new rapid NMR imaging method is presented (i) with optimized SNR, (ii) with the choice of a variable compromise between spatial, time resolution, and SNR, and (iii) with the possibility of recording NMR movies. Furthermore, the FLASH imaging sequence may easily be modified to allow three-dimensional NMR imaging by replacing the slice-selective rf pulse by a nonselective pulse and the slice selection gradient by an additional phase-encoding gradient perpendicular to the other gradients. 3D NMR images with a resolution of $128 \times 128 \times 128$ pixels may be obtained within a measuring time of about 4 min (*17*). However, a major advantage of the rapid 2D technique is the absence of motional artifacts within the images. Even dynamic imaging of rapid nonperiodic movements becomes possible (*18*) and fast physiological changes may be investigated by recording NMR "movies" comprising sequential images (*19*). When combined with rapid image reconstruction and display routines, sequential multislice FLASH images may be used to move the imaging plane "on line" through the body. In medical applications rapid NMR imaging will considerably improve the convenience

FIG. 4. Elimination of motion artifacts by FLASH NMR imaging. The images shown (128×128 pixels corresponding to 1 mm resolution, 4 mm slice thickness) refer to horizontal slices through the abdomen of a live anesthesized rabbit depicting a kidney, the lungs, the diaphragm, the stomach, and parts of the liver and the dorsal mediastinum. This cross section is affected by peristaltic, respiratory, and cardiac motions. (a) Conventional FLASH image with a measuring time of 2.3 s. From (b–d) as well as from (e–g) the measuring time increases from 9 s (b, e), to 18 s (c, f) and 36 s (d, g). The images (b–d) are obtained by increasing the repetition time, whereas the images (e–g) refer to averages of 4, 8, and 16 subsequent recordings of 2.3 s FLASH images, respectively.

of patients as well as lower the economic constraints to the use of NMR by today's public health care.

ACKNOWLEDGMENTS

Financial support by the Bundesminister für Forschung und Technologie (BMFT) of the Federal Republic of Germany (Grant 01 VF 242) is gratefully acknowledged.

REFERENCES

1. P. MANSFIELD AND P. G. MORRIS, *in* "Advances in Magnetic Resonance" (J. S. Waugh, Ed.), Suppl. 2, "NMR Imaging in Biomedicine," Academic Press, New York, 1982.
2. R. J. ORDIDGE, P. MANSFIELD, M. DOYLE, AND R. E. COUPLAND, *Br. J. Radiol.* **55,** 729 (1982).
3. J. HENNIG, A. NAUERTH, AND H. FRIEDBURG, *Magn. Reson. Med.*, **2,** in press (1985).
4. National Radiol. Protect. Board, *Br. J. Radiol.* **56,** 974 (1983).
5. J. FRAHM, A. HAASE, D. MATTHAEI, K. D. MERBOLDT, AND W. HÄNICKE, *J. Magn. Reson.* **65,** 130 (1985).
6. J. FRAHM, K. D. MERBOLDT, W. HÄNICKE, AND A. HAASE, *J. Magn. Reson.* **64,** 81 (1985).
7. German Patent Application P 3504734.8 (February 12, 1985).
8. A. HAASE, J. FRAHM, D. MATTHAEI, K.-D. MERBOLDT, W. HÄNICKE, Book of Abstracts, 4th Annual Meeting of the Society of Magnetic Resonance in Medicine, London, August 19–23, 1985, p. 980.
9. W. A. EDELSTEIN, J. M. S. HUTCHISON, G. JOHNSON, AND T. REDPATH, *Phys. Med. Biol.* **25,** 751 (1980).
10. P. A. BOTTOMLEY, W. A. EDELSTEIN, W. M. LEUE, H. R. HART, J. F. SCHENCK, AND R. W. REDINGTON, *Magn. Reson. Imaging* **1,** 69 (1982).
11. R. ERNST, *Adv. Magn. Reson.* **2,** 1 (1966).
12. J. S. WAUGH, *J. Mol. Spectrosc.* **35,** 298 (1970).
13. D. I. HOULT, *J. Magn. Reson.* **26,** 165 (1975); **35,** 69 (1979).
14. P. C. LAUTERBUR, *Nature* **242,** 190 (1973).
15. A. KUMAR, D. WELTI, AND R. R. ERNST, *J. Magn. Reson.* **18,** 69 (1975).
16. D. MATTHAEI, J. FRAHM, A. HAASE, W. HÄNICKE, AND K.-D. MERBOLDT, submitted.
17. J. FRAHM, A. HAASE, AND D. MATTHAEI, *J. Comput. Assist. Tomogr.*, in press.
18. J. FRAHM, A. HAASE, AND D. MATTHAEI, *Magn. Reson. Med.*, in press.
19. D. MATTHAEI, J. FRAHM, A. HAASE, AND W. HÄNICKE, *Lancet*, ii, 893 (1985).